14

Time-Resolved FTIR Difference Spectroscopy Reveals the Structure and Dynamics of Carotenoid and Chlorophyll Triplets in Photosynthetic Light-Harvesting Complexes

Alexandre Maxime and Rienk van Grondelle
VU University of Amsterdam
Netherlands

1. Introduction

Infrared spectroscopy is a very powerful tool to determine the chemical nature of molecules.

Differential infrared spectroscopy allows to select only those chemical vibrations involved in a light induced reaction. The structure and environment of unstable and short lived excited states can be probed by using step scan FTIR time resolved spectroscopy. In this chapter we present an application of time resolved FTIR step scan spectroscopy to the light harvesting complexes involved in the collection of solar energy in photosynthesis. The time resolved data are analysed using a global and target analysis procedure which allows identification of the dynamic and the spectral properties of short lived intermediates such as triplet states. Triplet state of chlorophyll a (Chl a) can react with oxygen and lead to the formation of singlet oxygen. Carotenoids avoid this reaction via triplet excitation energy transfer (TEET) and quench the triplet of Chl a. The peridinin chlorophyll protein (PCP), an algal light harvesting complex, which binds Per and Chl a is a good system to study photoprotection mechanism by infrared spectroscopy. Indeed Per and Chl a have both conjugated carbonyl groups that are efficient probes of the molecular state in the infrared. We first investigated by step scan spectroscopy the TEET reaction of Per and Chl a in solvent to get their respective spectral signature. Such a study leads to the identification of several mechanisms associated with the formation of triplet states in solution. Secondly the triplet formation is observed in two different PCP complexes leading to the unexpected conclusion that the Per triplet state is delocalised over the Chl a. In a third part we reveal that the same process of triplet sharing between Chl and carotenoid is also present in higher plants, in sharp contrast with purple bacteria for which the triplet is fully localised on the carotenoid. Our finding strongly suggests that in higher plants and algae a much stronger interaction between carotenoids and chlorophylls is at the basis of photoprotection, and represents an example of molecular adaptation in oxygenic photosynthesis.

2. Differential FTIR spectroscopy and data analysis

2.1 Time-resolved infrared spectroscopy

To gain information about the dynamics of the system time-resolved infrared spectroscopy has to be used. Characterization of unstable and short-lived reaction intermediates is required to understand the photo-chemical reactions of light harvesting systems. To investigate the dynamics of such systems time-resolved pump-probe spectroscopy is required. Two different time-resolved infrared (trIR) techniques are commonly used namely ultrafast midIR and step scan FTIR spectroscopy.

In these cases the light-induced difference of infrared absorption (ΔOD) of a sample is measured as a function of time. Then, the ΔOD signal at a given wavenumber and at a given delay time between the pump and the probe, ΔOD(υ,t), is given by:

$$\Delta OD(\upsilon,t) = OD(\upsilon,t)_{Light} - OD(\upsilon)_{Dark} = -\log\frac{I(\upsilon,t)_{Light}}{I(\upsilon)_{Dark}} \quad (1)$$

TrIR can provide many molecular details of the reaction mechanism of protein, associated with their specific lifetimes, which are complementary to X-ray and NMR structure analysis, such as:

- the electronic, redox, protonation and conformational state of the chromophore.
- the H-bonding, the protonation, the charge distribution of side chains of protein residues.
- the H-bonding state of the C=O and C-N-H involved in the peptide bond of the protein backbone which give informations about secondary structure dynamics and the propagation of structural changes.
- the H-bonding state of water molecules which are as essential as the side chain of the residues in achieving protein function in photoreceptors (Garczarek and Gerwert 2006).

Ultrafast midIR and step scan FTIR spectroscopy are complementary. On the sub-nanosecond time scale most of the reaction is confined to the chromophore and the neighboring amino acid residues in the binding pocket and can be monitored using ultrafast IR spectroscopy. Long lived excited states such as triplet state, side chain (de)protonation and large scale protein motion involving changes in secondary-tertiary structure of the protein generally take place on the nanosecond to millisecond time scale and can be monitored using step scan FTIR spectroscopy. In this chapter step scan spectroscopy will be described in detail.

2.2 Step scan-Time resolved FTIR spectroscopy

Step scan-Time resolved FTIR spectroscopy allows monitoring molecular reaction mechanism of proteins at longer time-scales than ultrafast IR spectroscopy. The absorbance changes can be monitored with time resolutions down to nanoseconds and followed for time periods ranging over nine orders of magnitude. The technique has already been successfully applied to the light-driven proton pump bacteriorhodopsin (Kotting and Gerwert 2005), the photosynthetic reaction center and the GTPase Ras (Kotting 2005), PYP (Brudler, Rammelsberg et al. 2001) and Appa (Majerus, Kottke et al. 2007). In contrast to

ultrafast mid-IR which uses a spectrograph containing a grating to disperse the probe beam on a 32-element MCT detector, Fourier-Transform Infrared (FTIR) spectroscopy is an interferometric method. The FTIR spectrometer consists of an infrared source, an interferometer, the sample, and the infrared detector. The interferometer is the heart of the spectrometer and consists in its simplest form of a beam splitter, a fixed mirror, and a moving mirror scanning back and forth. Therefore, the spectrum is not directly measured but its interferogram, i.e. the IR intensity reaching the detector as a function of the mirror position. The spectrum is subsequently obtained by Fourier transformation of the interferogram. The major advantages of FTIR spectroscopy, as compared to conventional dispersive IR spectroscopy, are the so-called multiplexing advantage (Felgett advantage) and the high energy flux reaching the detector (Jacquinot advantage), allowing rapid spectrum acquisition at a high signal to noise ratio. In the step-scan mode, the interferometer moving mirror may be visualized as being held stationary at the interferogram mirror position x_n. The protein activity is initiated, by a laser flash, and the time dependence of the intensity change at this interferogram position x_n is measured. Then the interferometer "steps" to the next interferogram data position x_{n+1}, and the reaction is repeated and measured again. This process is continued at each sampling position of the interferogram.

2.3 Data analysis for time-resolved infrared spectra. Global and target analysis

TrIR experiments result in a 3-dimensional dataset as the changes in intensity ($\Delta OD(\upsilon,t)$) are measured as a function of time and wavelength. A typical dataset results in ~20 000 data points. To analyze such large amounts of data a Global analysis procedure is required (van Stokkum, Larsen et al. 2004). Global analysis implies a simultaneous analysis of the entire 3-dimensional dataset which gives a correlation between different wavelength-regions and time scales. The total dataset is a superposition of contributions from different species (components) having their own time constants (lifetime). Description of such a total dataset should be obtained with a minimum amount (i) of time constants (k_i) that result in a good quality fit. Each component starts with a given concentration (c_i) that decays in time and possesses its own specific time-independent spectrum (ε_i). Mathematically, the observed signal S at any given time (t) or wavenumber (υ) can be described with:

$$S(\upsilon,t) = \sum_{i=1}^{n} c_i(t) * \varepsilon_i(\upsilon) \tag{2}$$

with $c_i = e^{(-k_i t)}$

The resulting spectra ε_i may represent mixture of known physico-chemical species and then do not contain directly physically relevant information. In such case decisions have to be made about a model that not only describes the raw data, but also generates relevant and meaningful spectra. Data previously obtained using different experimental techniques can be helpful in such context. The simplest model describing the measured data has to be chosen. The simplest model templates are the sequential and parallel models (Figures 1A and 1B) where one compartment flows directly into the next compartment with increasing lifetimes or to the ground state, respectively. A compartment represents a spectroscopic distinct state or physico-chemical species and symbolizes a component of the reaction with

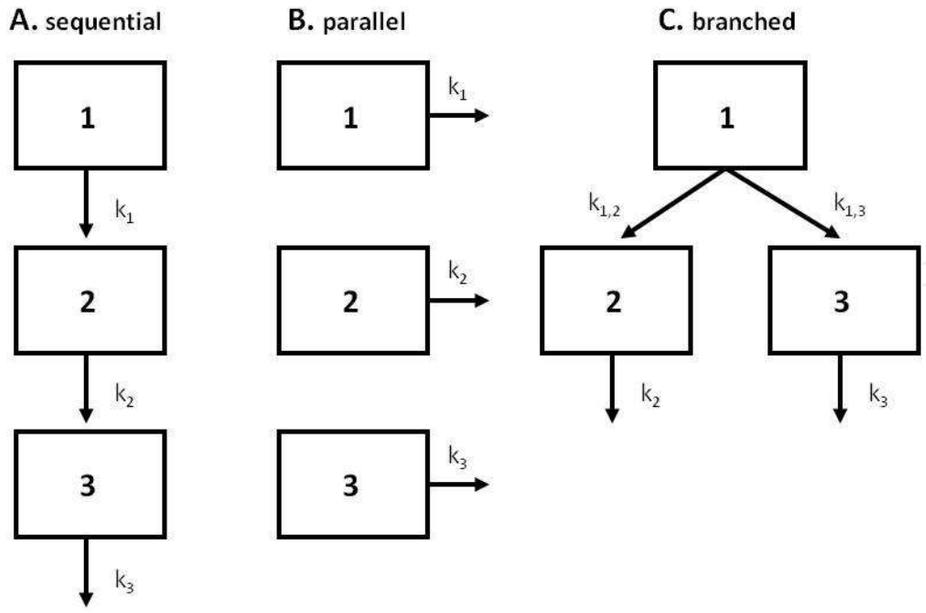

Fig. 1. Schematic view of a sequential model (A), a parallel model (B) and a branched scheme (C).

its spectrum (ε_i) and associated lifetime (k_i). Spectra that result from the application of a sequential and parallel model are called evolution associated difference spectra (EADS) and decay associated difference spectra (DADS), respectively. EADS estimated by a sequential model may represent mixtures of coexisting molecular states, since the possibility of branched or parallel dynamics are not taken into account. In order to disentangle the contributions a more complicated model must be used such as a branched model (Figure 1C), where one compartment can populate two other compartments. If one data set is analyzed with the three described models, then the resulting spectra for each compartment are different, except for compartment 1. Using a model different from the sequential or the parallel model is called a target analysis and can only be done if the data allows for it and/or if additional information is available from other techniques. In this latter case the spectra are no longer called DADS or EADS but species associated difference spectra (SADS).

3. Carotenoid and chlorophyll triplet state dynamic

3.1 Photoprotection mechanisms in Peridinin chlorophyll proteins. The chlorophyll triplet quenching by peridinin

Photosynthesis is the process by which some terrestrial and marine organisms acquire energy from sunlight and transform it into chemical energy (organic compounds) (Gest 2002). Life on earth began roughly ~3.8 billion years ago (Schopf 1992), with some cyanobacterial species being the first photosynthetic organisms to appear. Accumulation of oxygen in our atmosphere has thus been possible due to the presence of these organisms, capable of performing oxygenic photosynthesis. Later the appearance of higher plants led to the production of organic compounds which constitute the basic source of energy for most living organisms. The photosynthetic process and, therefore the abundance and diversity of

life on Earth, ultimately depends on the energy provided by the Sun. Photosynthetic organisms use antenna pigment-proteins to harvest light. Absorbed solar energy is transferred to the reaction center (RC) where it is converted into an electrochemical gradient, which is used to synthesize ATP, powering the cell (van Grondelle, Dekker et al. 1994). Together with (Bacterio)Chlorophyll ((B)Chl) carotenoids are the main pigments of photosynthesis. In addition to their structural involvement in the antenna architecture, carotenoids have a dual function namely light harvesting and photoprotection (Frank and Cogdell 1996). They harvest light in the blue –green spectral region where (B)Chl absorbs weakly thus increasing the absorption cross-section of the light harvesting system where sunlight is optimal. Carotenoid excitation is followed by ultrafast energy transfer to (B)Chl with a high efficiency (Shreve, Trautman et al. 1991; Ritz, Damjanovic et al. 2000; Walla, Linden et al. 2000; Zhang, Fujii et al. 2000; Papagiannakis, Kennis et al. 2002; Holt, Kennis et al. 2003; Zigmantas, Hiller et al. 2004). (B)Chl intersystem crossing (ISC) may lead to triplet formation, the efficiency of which depends on the singlet excited state lifetime. The long-lived (ms timescale) (B)Chl triplet reacts with ground state oxygen (which is a triplet state) to produce the highly reactive oxygen singlet ($^1O_2$) (Krieger-Liszkay 2005). In light harvesting complexes (LHC), this process competes with fast (ns timescale) (B)Chl triplet excitation energy transfer to the carotenoid thereby (Krieger-Liszkay 2005) avoiding formation of $^1O_2$ and ultimately the destruction of the light harvesting apparatus. In addition, carotenoids are also able to scavenge singlet oxygen.

Singlet oxygen can be formed by the quenching of chlorophyll triplet states:

^{3}Chl-*a** + $^3O_2 \rightarrow$ Chl-*a* + $^1O_2^*$ (singlet oxygen formation)

To prevent this reaction, carotenoids with their low-lying triplet states quench long-lived chlorophyll triplets (Nagae, Kakitani et al. 1993; Frank and Cogdell 1996; Krueger, Scholes et al. 1998; Krueger, Scholes et al. 1998; Damjanovic, Ritz et al. 1999; Damjanovic, Ritz et al. 2000) and scavenge singlet oxygen (Cogdell, Howard et al. 2000):

^{3}Chl-*a** + Car $\rightarrow$ Chl-*a* + ^{3}Car* (chlorophyll triplet quenching)

$^1O_2^*$ + Car $\rightarrow$ $^3O_2$ + ^{3}Car (singlet oxygen scavenging)

In PCP, the triplet states of Chl-*a* are formed *via* intersystem crossing (ISC) from Chl-*a* singlet states. The latter are formed after direct Chl-*a* excitation or after excitation energy transfer (EET) which follows direct excitation of Per (Bautista, Hiller et al. 1999; Krueger, Lampoura et al. 2001; Zigmantas, Hiller et al. 2002). The Per triplet states are populated by triplet excitation energy transfer (TEET), which is governed by an electron-exchange interaction (Dexter mechanism) (Dexter 1953; Cogdell and Frank 1987). The PCP visible T-S spectra (Carbonera, Giacometti et al. 1996; Kleima, Wendling et al. 2000) exhibit a Q_y Chl-*a* differential signal assigned to Chl-*a*-carotenoid interaction and is similar to carotenoid T-S spectra found in bacterial and higher plant antennae (Van der Vos, Carbonera et al. 1991; Angerhofer, Bornhauser et al. 1995; Peterman, Dukker et al. 1995). This interaction signal shows concerted dynamics with the carotenoid triplet (Peterman, Dukker et al. 1995; Kleima, Wendling et al. 2000) and has been discussed in terms of a Stark effect, but its exact nature remains unclear. It is then of interest to investigate such triplet dynamic using microsecond time-resolved FTIR spectroscopy to measure triplet formation in PCP by monitoring excitation-induced variations in the vibrational modes of the chromophores. For

infrared spectroscopy a good model to study this photoprotection mechanism is the water soluble LHC from the dinoflagellate *Amphidinium carterae*, A-PCP. Indeed it binds only one type of carotenoid and chlorophyll, Per and Chl a, respectively. In addition, Per and Chl-*a* possess conjugated carbonyl groups which are sensitive to the protein environment and the electronic state of the pigment. In other words, the carbonyl modes are the molecular probes for the pigments: the 9-keto mode of the Chl-*a* and the carbonyl group of the lactone ring of Per. The keto modes are generally expected at lower energies (≤ 1700 cm^{-1}) compared to lactone modes (> 1700 cm^{-1}) which makes them easily distinguishable.

The 2.0 Å crystal structure of A-PCP reveals a trimeric arrangement. The protein is mainly composed of α-helices structure and surrounds a hydrophobic cavity in which besides the pigments also two lipids are bound. The A-PCP monomer contains 2 Chlorophyll-*a* and 8 Peridinins. The molecular structures of Chlorophyll-*a* (Chl-*a*) and peridinin (Per) are shown Figure 2A and 2B. In each half of the PCP monomer one Chl-*a* is closely surrounded by 4 Per (Figure 2C) (Hofmann, Wrench et al. 1996; Hofmann 1999) leading to high efficiency for both light harvesting and photoprotection (Kleima 2000; Alexandre, Luhrs et al. 2007). The N- and C-terminal halves of the polypeptide to which the two clusters of pigments are bound form almost identical domains related by a pseudo two-fold symmetry axis. PCP most likely functions as a LHC that transfers its energy mainly to the PSII RC complex (Knoetzel and Rensing 1990; Mimuro, Tamai et al. 1990). Since the latter complex is located in the photosynthetic membrane, transfer has to occur from a water-soluble complex to a membrane bound complex. As no specific binding site has been identified so far, PCP could in principle either transfer its energy directly to the PSII RC or indirectly *via* the membrane bound Chl-a/c complex, which is an analog of LHCII of green plants. Per has a unique

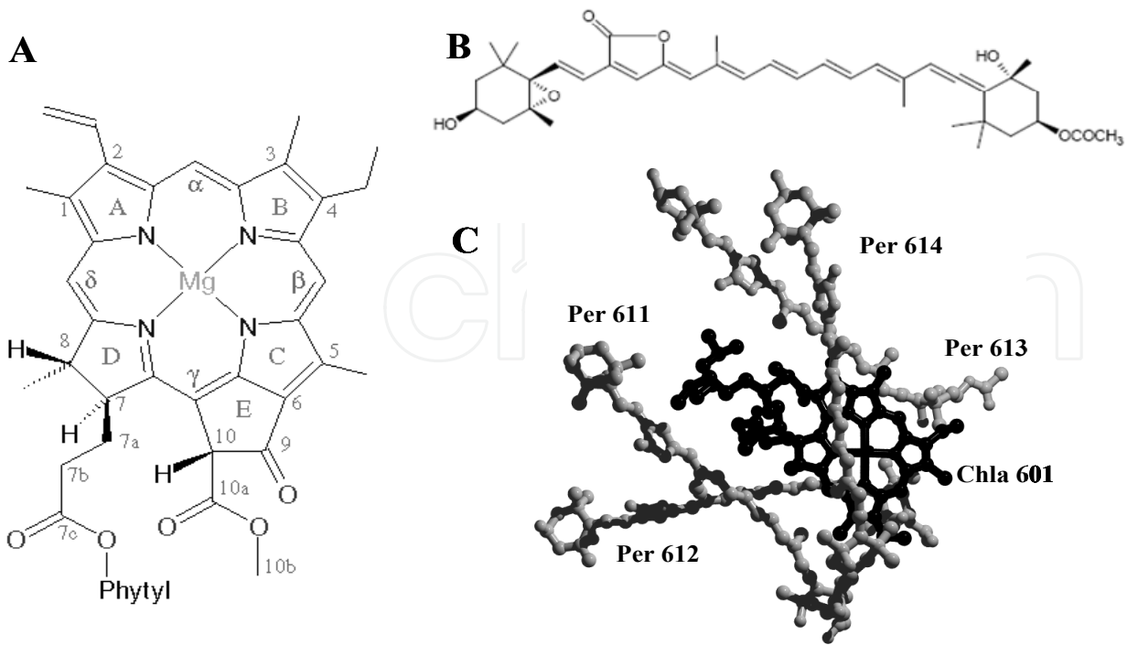

Fig. 2. Molecular structure of Chl-*a* (A) and Per (B). Pigments organization, one Chl-*a* (black) surrounded by 4 Per (grey) (C).

molecular structure constituted of an allene moiety and a lactone ring in conjugation with the π-electron system of the carotenoid backbone, an epoxy group with a secondary alcohol group on one beta-ring and an ester group located on the opposite beta-ring with a tertiary alcohol group (Figure 2B). The structural differences between Per and other carotenoids are most likely related to its specific function in PCP. In contrast to most photosynthetic LHCs, the carotenoid (Per), and not Chl-*a*, is the main light-absorbing pigment in PCP. Per's unusual structure and especially its conjugated lactone carbonyl confers a high plasticity of absorptivity and reactivity to this carotenoid, for instance by mixing CT states with the lower excited states (Bautista, Connors et al. 1999; Zigmantas, Hiller et al. 2002; Vaswani, Hsu et al. 2003; Ilagan, Shima et al. 2004; Zigmantas, Hiller et al. 2004; Premvardhan, Papagiannakis et al. 2005).

A different dinoflagellate species *Heterocapsa pygmaea* uses a LHC closely related to A-PCP, H-PCP. H-PCP has the same pigment stoichiometry as A-PCP but its peptide unit is about half the size of that of A-PCP and contains only half the number of pigments (Song, Koka et al. 1976; Norris and Miller 1994; Hiller, Crossley et al. 2001). The overall identity of the H-PCP monomer with that of the N and C terminal domains of A-PCP is about 70% (Hiller, Crossley et al. 2001). 3-D Modeling of the H-PCP sequence on the high-resolution x-ray structure of A-PCP has shown only major differences in the trimer interface (Hiller, Crossley et al. 2001). In nature, H-PCP is found as a dimer. Thus, the A-PCP monomer can be considered as the covalent equivalent of the H-PCP dimer and the pigment conformation in both systems should be very similar. This view is supported by the high similarity of the spectroscopic properties (Abs, CD, T-S spectra) of the two complexes (Carbonera, Giacometti et al. 1996).

3.2 Peridinin and chlorophyll triplet state in solvent

It is important to firmly establish our spectral assignment of Per and Chl-*a* modes in the ^{3}Per and ^{3}Chl-*a* states using an artificial system where Per and Chl-*a* are not strongly coupled. To this end, we performed step-scan time resolved FTIR measurements on Per mixed with Chl-*a* in organic solvent to observe TEET on the μs timescale and extract their individual spectra using global and target analysis. The two chromophores were mixed in THF with a stoichiometric ratio Per: Chl-*a* of 1:8 with a Chl-*a* OD (670 nm) of about 100 cm^{-1}. Time-resolved FTIR data has been obtained by direct excitation of Chl-*a* at 625 nm and the ensuing spectral evolution was analyzed using global and target analysis. Global analysis in terms of a sequential kinetic scheme shows that three components are required to fit the data. In order to determine the origin of the third component, we used target analysis. The best fit was obtained with a three level scheme, in which the first component decays in 3.5 μs in parallel to the second and the third component, which decay to the ground state in 7 μs and 3 ms, respectively. The kinetic model is displayed in Fig.3. The first component decays into the second and third components with an estimated yield of 60% and 12% respectively. About 28% of the first component amplitude is lost *via* triplet-triplet annihilation and decays to the ground state. Experiments with Chl-*a* only in THF confirmed that the first component decays into a component having similar lifetime and spectral features as compared to the third component observed in the mixed Chl-*a*/Per sample. We note that Per is unable to quench the third component which suggests that it can be assigned to a radical state of Chl-*a*. The three SADS that result from the target analysis of the mixed Chl-*a*/Per data are shown

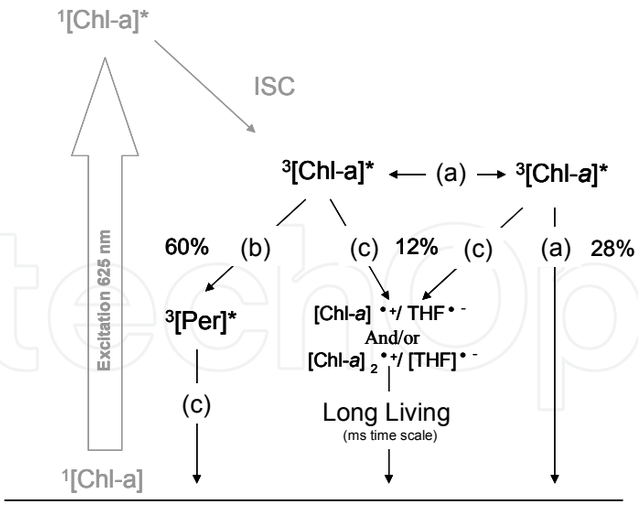

(a) Triplet-triplet annihilation proceeds with a yield of 28% (^{3}[Chl-*a*]* + ^{3}[Chl-*a*]* = ^{1}[Chl-*a*]* + ^{1}[Chl-*a*]). (b) Triplet excitation energy transfer from Chl-*a* to Per takes place in 3.5 µs with a yield of 60%. (c) Chl-*a* radical formation have a yield of 12%.

Fig. 3. Target analysis kinetic model applied to the time-resolved data of Per mixed with Chl-*a* in THF (excitation at 625 nm).

in Figure 4. The first component (SADS1), shown in black in Fig. 4, is assigned to ^{3}Chl-*a* and has a lifetime of 3.5 µs. Its short lifetime indicates that the ^{3}Chl-*a* is strongly quenched in the presence of Per. This SADS matches the FTIR triplet minus singlet (T-S) spectrum of Chl-*a* in THF at 90K (Breton, Nabedryk et al. 1999). Bands at 1747(-)/1733(+) and 1698(-)/1671(+) cm^{-1} are assigned to the Chl-*a* *10a*-ester and *9*-keto carbonyl, respectively. The *9*-keto carbonyl stretch of Chl-*a* in THF at 1698 cm^{-1} is non H-bonded and in a moderately polar environment.

In SADS1 (Fig. 4), the band at 1599 (-) cm^{-1} is typical of a 6-coordinated Chl-*a* Mg-atom (Fujiwara 1986; Fujiwara and Tasumi 1986; Groot 2004). If Chl-*a* is monomeric, then Chl-*a* will be 6-coordinated with two THF molecules ligated to the central Mg atom forming the complex [Chl-*a*]-[THF]$_2$. However the presence of a dip in the ESA at 1657 cm^{-1}, which is not present in the FTIR T-S spectra in ref.(Breton, Nabedryk et al. 1999), may indicate that the observed triplet state actually resides on aggregated Chl-*a*. Chl-*a* at high concentration in an apolar solvent, in the absence of water, is known to aggregate with a typical IR band near 1657 cm^{-1} for Chl-*a* dimers (Katz, Ballschmiter et al. 1968). The aggregation most likely follows from the high concentration used for the FTIR experiments of about 1 mM (OD at 670 nm of about 100 cm^{-1}) in THF. Assuming that Chl-*a* is dimeric in our sample, the 1657 cm^{-1} band most likely indicates a second Chl-*a* (Chl-*a*2) with its 9-keto bound to the Mg atom of the first Chl-*a* (Chl-*a*1) (Katz, Ballschmiter et al. 1968; Fujiwara 1986). As SADS1 is dominated by modes of Chl-*a*1, this suggest that the triplet state is mainly localized on this Chl-*a* for which the ester and keto are free of (H-) bonding.

The second SADS rises in 3.5 µs and decays in 7 µs. It is assigned to ^{3}Per (dash-dot gray SADS in Fig. 3) according to its characteristic decay time. ^{3}Per is formed *via* TEET from ^{3}Chl-*a*, note that this component is not observed in Chl-*a* only samples in THF. The ^{3}Per SADS is dominated by a band-shift at 1761(-)/1733(+) cm^{-1}, assigned to the C=O lactone stretch of

Per. Thus, C=O lactone conformers in THF, which is moderately polar and aprotic, are relatively homogenous and non H-bonded with a main frequency at 1761 cm^{-1}.

In SADS2, the small amplitude bandshift observed around 1697(-)/1666(+) cm^{-1} arises from a contribution by SADS1 (i.e. ^{3}Chl-*a*) that the target analysis fails to fully remove due to our limited time resolution, S/N ratio and baseline fluctuations. A Chl-*a* – Per sample at a 1:1 stoichiometric ratio (OD_{670} = 150 cm^{-1}) exhibits a shorter ^{3}Chl-*a* lifetime of about 1 µs. Target analysis resulted in a ^{3}Per SADS (SADS-Per) almost free of ^{3}Chl-*a* contributions. By comparing this latter SADS-Per with SADS2 (Figure 4, light gray line) we can confirm that in SADS2 (Figure 4) the small amplitude bandshift observed around 1697(-)/1666(+) cm^{-1} follows from a spurious contribution from SADS1 (^{3}Chl-*a*).

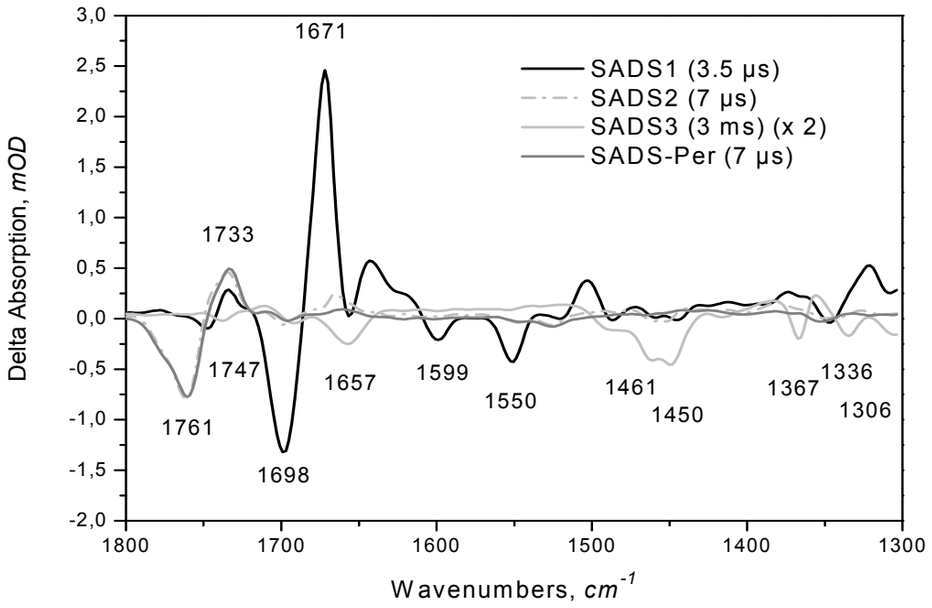

Fig. 4. SADS resulting from target analysis applied to data obtained upon direct Chl-*a* excitation at 625 nm of Per and Chl-*a* mixed in THF with a stoichiometric ratio Per: Chl-*a* of 1:8 with a Chl-*a* OD at 670 nm of about 100 cm^{-1}. The black spectrum is assigned to ^{3}[Chl-*a*]*, it decays in 3.5 µs into the dash-dot gray and light gray SADS. The dash-dot gray SADS is assigned to ^{3}[Per]* and decays to the ground state in 7 µs. The light gray SADS contains signature of Chl-*a* cation and THF radical anion; it decays in 3 ms. The gray spectrum (SADS-Per) is obtained upon direct Chl-*a* excitation at 625 nm of Per and Chl-*a* mixed in THF with a stoichiometric ratio Per: Chl-*a* of 1:1 with a Chl-*a* OD at 670 nm of about 150 cm^{-1}.

The third SADS has an overall low amplitude. It is assigned to the Chl-a^+/THF^- radical pair which is formed with a relatively low yield from the ^{3}Chl-*a* and decays with an estimated lifetime of 3 ms. In the carbonyl region, the third SADS exhibits up-shifted ester and keto C=O stretch frequencies at 1738(-)/1751(+) and 1692(-)/1712(+), 1657(-)/1680(+) cm^{-1}, characteristic for radical cation formation (Breton, Nabedryk et al. 1999). The presence of

two different 9-keto stretches confirms our earlier hypothesis that a Chl-*a* dimer (Chl-*a*1/Chl-*a*2) is present under these conditions. In contrast to the triplet state, which seemed to be mainly localized on Chl-*a*1 (SADS1), the radical appears to be delocalized over the two Chl-*a* molecules of the dimer, as its infrared signature is in fact similar to $P700^+$ in the Photosystem I RC (Breton, Nabedryk et al. 1999). Below 1500 cm^{-1} new bands have appeared in SADS3. A strong negative band with a double peak character is observed centered at 1450 and 1461 cm^{-1} in addition to bands at 1367, 1336 and 1306 cm^{-1}. These bands are typical for THF (data not shown) and up-shifted after Chl-*a* excitation to 1630-1515, 1382, 1354 and 1321 cm^{-1}, respectively. Such up-shifts indicate radical formation of THF, probably the radical anionic ([THF]•-) state, forming the [Chl-*a*]•+/[THF]•- radical pair.

3.3 A PCP triplet state dynamic

In this section we use microsecond time-resolved FTIR spectroscopy to measure triplet formation in PCP by monitoring excitation-induced variations in the vibrational modes of the PCP chromophores. In the following paragraphs, we present the estimated lifetimes, the decay associated difference spectra (DADS) and the vibrational mode assignment of three sets of time-resolved IR data resulting from excitation of Chl-*a* at 670 nm (Q_y), and Per at 480 nm (maximum of Per absorption) and 530 nm (red edge of Per absorption, Fig.5). Excitation at 550 nm gave essentially the same result as 530 nm (data not shown).

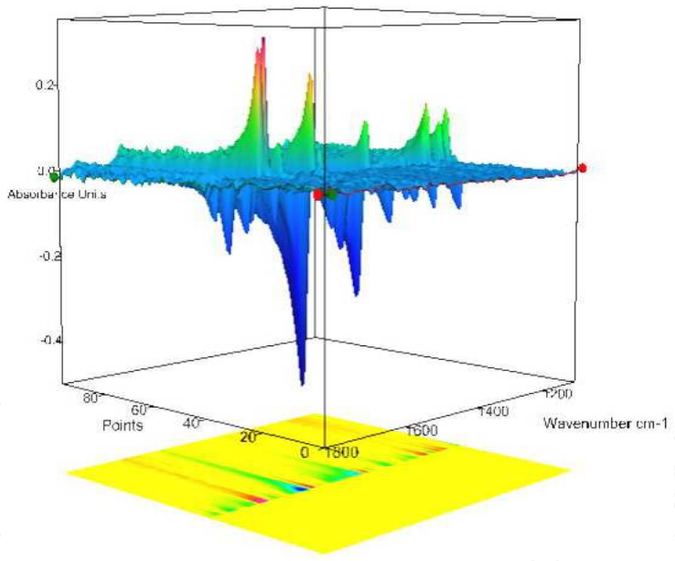

Fig. 5. Differential absorbance signals of PCP obtained by step-scan Fourier-transform infrared spectroscopy. Raw data with 5 µs time resolution for 530 nm excitation; intensity 2 mJ/cm^2.

Time-resolved mid-IR spectra were collected (Fig. 6A) and globally analyzed at frequencies between 1100 and 1800 cm^{-1}, and the resulting decay associated difference spectra (DADS) are shown in Fig. 6B. To describe the time resolved data, we used a parallel model, which required three components: two fast lifetimes, of the order of tens of microseconds and a longer one that we do not consider further We find the triplet state dynamics of PCP at RT to be described by lifetimes of 13 and 42 µs which are typical of carotenoid triplets. Previous

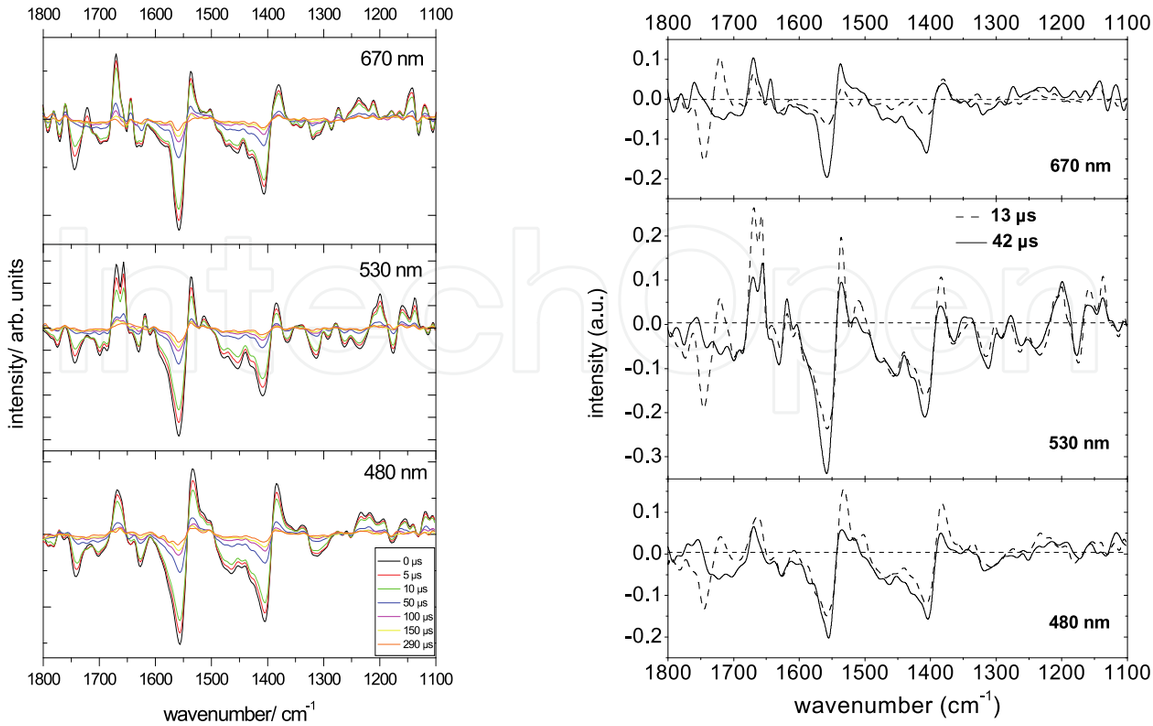

Fig. 6. (A) Time slices of raw data at different excitations. (B) DADS of PCP obtained using a parallel model after different excitations. DADS1 (dotted line) and DADS2 (black line) are associated with a 13 and 42 µs lifetime, respectively.

experiments on PCP in the visible spectral region reported one Per triplet lifetime of 10 µs at RT (Bautista, Hiller et al. 1999; Kleima, Wendling et al. 2000) and two lifetimes of 13 and 40 µs at 77 K (Kleima, Wendling et al. 2000) and 13 and 58 µs up to 200 K (Carbonera, Giacometti et al. 1999), respectively. In Fig. 6 the positive DADS signals originate from excited state absorption (ESA) of the triplet states, and negative DADS signals from the bleach of the ground state.

3.3.1 Spectral analysis

In our spectral analysis, we distinguish four regions of interest: The carbonyl region (1800-1630 cm^{-1}); the C=C stretch region, characteristic of the polyene backbone of carotenoids and chlorophylls giving rise to bands between 1610 and 1525 cm^{-1}; the CH-deformations and possible lactone-ring modes in the region of 1450-1380 cm^{-1} and the fingerprint region below 1380 cm^{-1} with e.g. CH-out-of-plane, C-C and C-O stretches and their combinations.

As we can see in Fig. 6B, the two DADS show many spectral similarities. The weak bands at 1623,1633 cm^{-1} (bleach) and strong bands at around 1555/1530 cm^{-1} (bleach/ESA) are Per C=C stretching modes. Typically, carotenoid C=C stretching modes are around 1520 cm^{-1} – e.g. spheroidene, ß-carotene (Noguchi, Hayashi et al. 1990; Hashimoto, Koyama et al. 1991) – and down-shifted by 20 cm^{-1} to around 1500 cm^{-1} in the T_1 state (Hashimoto, Koyama et al. 1991). In Per we observe slightly higher frequencies, indicating a decrease in bond-order, as observed normally for peripheral C=C stretches (Nagae, Kuki et al. 2000). Moreover, the broad band extending from ~1480 cm^{-1} to lower frequencies (bleach) due to CH-deformation

modes is characteristic of carotenoids (Bernhard and Grosjean 1995). The reported modes of Chl-*a* in PCP (Kleima, Wendling et al. 2000) at 1610, 1553 and 1526 cm^{-1} might also contribute to these bands to a minor extent. Additional recognizable modes are at ~1450 cm^{-1} the methylene C-H deformation and the methyl asymmetric bending modes, as well as the symmetric methyl bending mode of the Per backbone peaks at 1408/1380 cm^{-1} (bleach/ESA) (Bernhard and Grosjean 1995).

Carbonyl region – molecular probes

The carbonyl region contains contributions from Per and Chl-*a* since both have carbonyl groups in conjugation with their electronic system. These carbonyl modes are very sensitive to electronic changes and can be used as molecular probes for the individual chromophores. The carbonyl modes that can be expected in this region are the lactone mode of Per, and the 10a-ester and 9-keto modes of Chl-*a* (Fig. 7).

After global analysis, the DADS in the carbonyl region show five major frequencies in the ground state bleach (best resolved with 530 nm excitation): 1745 cm^{-1} (DADS1), 1741, 1720 cm^{-1} (DADS2), 1699 and 1686 cm^{-1} (both DADS) as seen Figure 7.

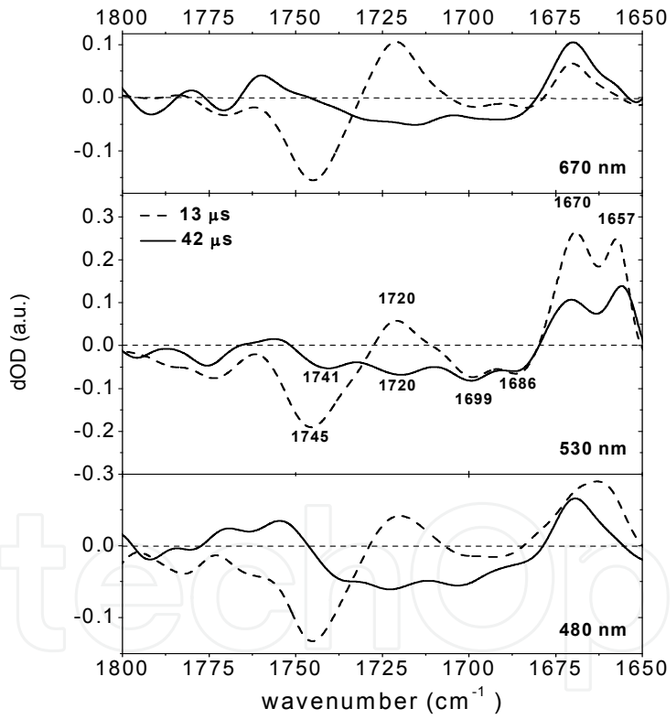

Fig. 7. Comparison of the carbonyl modes of the PCP DADS at 670, 530 and 480 nm excitations.

Carbonyl modes of Chl-a

The bands at ~1699, 1686 cm^{-1} (bleach), shown in Fig. 6 and 7, match the 1697 and 1681 cm^{-1} ones reported from fluorescence line narrowing (FLN) spectra at 4 K (Kleima, Wendling et al. 2000). The ESA of the two bands has shifted down to 1670 and 1657 cm^{-1}, respectively. Such a down-shift is typical for the 9-keto vibration of Chl-*a* in T-S FTIR spectra and can be

perfectly overlapped with the T-S FTIR spectrum of Chl-*a* in THF (Breton, Nabedryk et al. 1999). Chl-*a* triplets are known to exhibit a down-shift in the ESA, while Chl-*a* cations are up-shifted (Breton, Nabedryk et al. 1999; Breton 2001; Noguchi 2002). A hypothetical charge transfer state leading to Per (+)/Chl-*a*(-),would be expected to downshift the 9-keto vibration of Chl-*a* anion by about 55 to 92 cm^{-1} as observed for BPheo/BPheo$^-$ in THF (Mantele, Wollenweber et al. 1988), Pheo/Pheo$^-$ in PSII (Okubo and Noguchi) and BChl-a/BChl-a$^-$ (Hartwich, Geskes et al. 1995). In our data the 9-keto vibration of Chl-*a* down shifts by 30 cm^{-1} and strongly suggests that only Chl-*a* triplets exist on typical triplet carotenoid lifetimes and we can exclude the presence of Chl-*a* cations and anions. From the 9-keto-mode-amplitudes at 1699, 1686 cm^{-1}, we conclude that both Chl-*a* molecules of the quasi-symmetric PCP monomer are involved in the triplet state dynamics at RT, however, to a different extent depending on the excitation wavelength. The 9-keto mode is the strongest mode in T-S Chl-*a* FTIR difference spectra, about three times more intense than the 10a-ester mode (Breton, Nabedryk et al. 1999; Breton 2001), so we assign the other strong carbonyl modes to the lactone vibration of Per.

Carbonyl modes of Per

The remaining three ground state bleach modes – again best resolved after 530 nm excitation– at 1745 cm^{-1} (DADS1), 1741 (DADS2) and 1720 cm^{-1} (DADS2) represent the lactone carbonyl modes of three distinguishable Per conformers; however the 1741 cm^{-1} (DADS2) conformer is absent under 670 nm excitation. (Fig. 7) The Per ester group, which could be a possible candidate for these frequencies is located at one of the cyclo-hexane end-groups, and isolated from the conjugated backbone. For this reason, we do not expect contributions of the ester group after electronic excitation. The carbonyl-stretch of a five-membered lactone has a typical frequency of 1765±5 cm^{-1} (Kristallovich, Shamyanov et al. 1987), which can downshift by 20 cm^{-1} in conjugation with a π-system, as in Per, and even further in a polar environment or with hydrogen bonding of the carbonyl to the protein pocket. Moreover, the 25 cm^{-1} down-shift of the ESA corresponding to the 1745/1720 cm^{-1} bands would be large compared to 5 cm^{-1} for ester groups (as reported e.g. for chlorophyll) (Breton 2001). The observed ground state bleach modes are in agreement with Per resonant (530 nm) Raman data for PCP (unpublished data, Papagiannakis, E. and Robert B.) which display only two broad bands at 1745 and 1720 cm^{-1} in the carbonyl region. In addition, the resonant Raman spectrum of Per in methanol shows only one broad carbonyl frequency peaking around 1740 cm^{-1}.

The spectral assignments leads to the conclusions that:

- several conformers are involved in the triplet decay dynamics with bands at 1745, 1741, 1725 cm^{-1} and bands at 1695 and 1681 cm^{-1} assigned to various Pers and Chl-*a* conformers, respectively, experiencing different protein environment.
- Differential signals of Per and Chl-*a* are characteristic for their respective triplet states, which disappear with typical carotenoid triplet decay time constants. This implies that in PCP, while the triplet is on the Per, the triplet wavefunction is delocalised over the Chl-*a*, and both triplet signals decay with typical carotenoid tripet lifetimes.
- In addition, both Per and Chl-*a* infrared differential signals show an excitation wavelength dependence. The low frequency keto carbonyl Chl-*a* is more populated and the 1741 cm^{-1} Per conformer appears in DADS2 upon direct red Per excitation (530 and/or 550 nm) in comparison to direct Chl-*a* excitation (670 nm). The 1720 cm^{-1}

dynamics shows a strong wavelength dependence suggesting increased population of this Per conformer upon direct Per excitation. These spectral changes are accompanied by an overall increase of signal amplitude observed from 670 to 480 and to 530 nm. This wavelength dependence indicates that Per triplet formation proceeds via different pathways.

3.4 Triplet quenching in HPCP

It is of interest to investigate whether the same "triplet sharing" occurs in H-PCP as observed in A-PCP. In A-PCP, we previously observed the coexistence of Per and Chl-*a* carbonyl modes during the Per triplet lifetimes of 13 and 42 μs (Alexandre, Luhrs et al. 2007), which led us to conclude that in this triplet state, ^{3}Chl-*a* and ^{3}Per are mixed. Here, we investigated the H-PCP complex by step scan time-resolved FTIR spectroscopy to assess the nature of its triplet state. Upon excitation of peridinin at 530 nm, the H-PCP triplet decay is satisfactorily fitted with a single time constant of 10 μs. Excitation of H-PCP at 670 nm gave essentially the same result (data not shown). Figure 8 shows the DADS with a 10 μs lifetime in H-PCP (black line), plotted along with the 13 μs DADS observed in A-PCP (gray line), reproduced from ref. (Alexandre, Luhrs et al. 2007). Note that in A-PCP, also a 42 μs decay component with a distinctly different infrared signature was observed in the step-scan FTIR experiment (Alexandre, Luhrs et al. 2007). The H-PCP triplet state is spectrally very similar to the triplet state of A-PCP that decays in 13 μs. In both complexes, specific Per C=O lactone conformers are involved in the triplet state, of which the 1745(-)/~1720(+) cm^{-1} is the principal signature. In H-PCP, the bands at 1745(-)/1724(+) are assigned to the Per C=O lactone, while the 1700(-)/1667(+) cm^{-1} shift is attributed to the Chl-*a* C=O 9-keto (Breton, Nabedryk et al. 1999), showing that in the H-PCP triplet IR spectrum, explicit ^{3}Chl-*a* modes are present. This result indicates that some Chl-*a*/Per specific conformations and interactions are conserved in both A-PCP and H-PCP to achieve the efficient photo-protective TEET. This is consistent with the similar T-S ODMR spectra obtained for both complexes (Carbonera, Giacometti et al. 1996). Thus we conclude that both in A-PCP and in H-PCP the triplet state is shared by Per and Chl-*a* in a similar fashion.

In the 10 μs DADS of H-PCP (Figure 8), at least two C=O lactone conformers (1745 and 1710 cm^{-1} in a relative stoichiometry of about 80 and 20%) can be identified for H-PCP, independent of the excitation wavelength. For A-PCP one or two conformers at 1745 and 1745-1725 cm^{-1} depending on the excitation wavelength have been observed, i.e. 670 and 480-530 nm for the 13 μs component (Alexandre, Luhrs et al. 2007). In the two components of A-PCP, three Per conformers have been identified with lactone carbonyl vibrations at 1745, 1741 and 1725 cm^{-1}. This is consistent with the observation that the Per bound to the protein in H-PCP and A-PCP adopts multiple conformations (Hofmann, Wrench et al. 1996). Excitation of A-PCP yielded two triplet decay components of 13 and 42 μs (Alexandre, Luhrs et al. 2007). The differences between A-PCP and H-PCP may be related to the different protein structure, i.e., H-PCP is a 15.5 kDa homo-dimer and A-PCP is a 32 kDa trimer. The 32 kDa unit of A-PCP is asymmetric, composed of two different N-terminal and C-terminal units that share 56% of identity (Hofmann, Wrench et al. 1996). In contrast, H-PCP is a symmetric homo-dimer. The asymmetry within the A-PCP monomer is responsible for the Chl-*a* singlet equilibration on a ps timescale (Kleima, Hofmann et al. 2000; Salverda 2003). Possibly, the asymmetry in A-PCP leads to the observed triplet populations with different lifetimes.

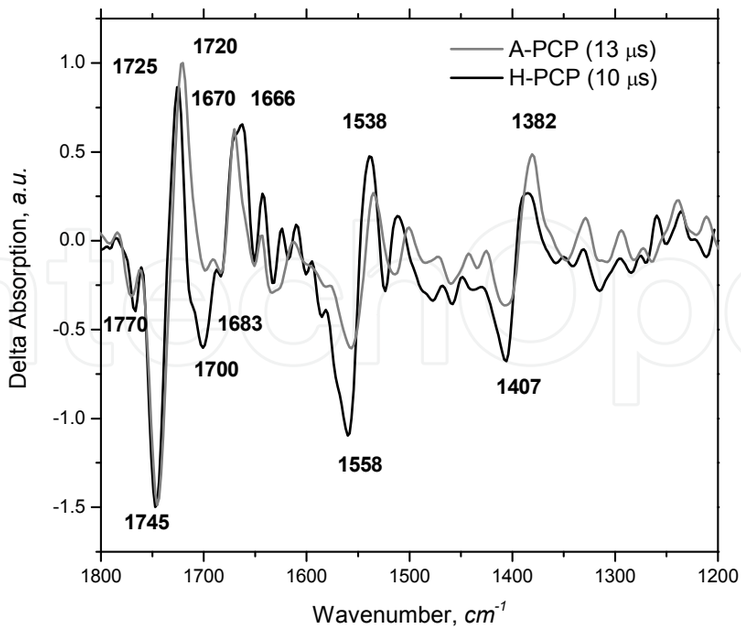

Fig. 8. Decay-Associated Difference Spectra (DADS) that result from a global analysis of step-scan FTIR data of H-PCP and A-PCP. The black line represents the 10 μs component in H-PCP. The gray line represents the 13 μs DADS in A-PCP.

The second component in A-PCP has been observed below 200 K by Carbonera *et al*. (Carbonera, Giacometti et al. 1999) and at 77K by Kleima *et al*., while only a 10 μs component was present at room temperature in the latter work (Kleima, Wendling et al. 2000). We reproduced Kleima's result at room temperature under aerobic and anaerobic conditions, by measuring the triplet decay in the visible using a diluted A-PCP solution. We found only the 10 μs component under aerobic and anaerobic conditions, which excludes an effect related to oxygen (data not shown). Thus, it seems that the appearance of the ~40 μs component is likely related to a protein conformational change induced by cooling and/or high concentrations used for FTIR, rather than a temperature effect on the equilibration among the triplet sublevels (Carbonera, Giacometti et al. 1999).

We previously proposed that the Per conformers involved in the photoprotective mechanism were likely Per 612/622 and Per 614/624. In a recent TR-EPR study (Di Valentin, Ceola et al. 2008), participation of the Per 612/622 pair in the ^{3}Chl-*a* quenching was considered unlikely on the basis of the similarity of the ^{3}Per triplet spectra in Main Form A-PCP (MFPCP) and High Salt A-PCP (HSPCP), since the latter does not bind the Per 612/622 pair. Comparison between experimental and calculated EPR spectra led the authors to conclude that the triplet was mainly (~80%) localized on the Per 614/624 pair, which has the shortest center-to-center distance to the Chl-*a*. This conclusion is consistent with the result of MD calculations showing that in the triplet state, the highest spin density is localized in the center of the Per backbone (Di Valentin, Ceola et al. 2008). Thus, it seems likely that in the step-scan FTIR experiments, the main Per conformer at 1745(-)/~1720(+) cm^{-1} corresponds to Per 614, Per 624, or both. Hence, we conclude that in A-PCP and H-PCP, Per 614 and/or 624 likely constitute the principal ^{3}Chl-*a* quenchers, and that their specific interaction with Chl-*a* promotes the mixing of the ^{3}Chl-*a* and ^{3}Per states during the lifetime of ^{3}Per.

3.5 Triplet state in higher plants

It has been recently reported that the TEET in LHCII takes place in less than 4 ns and is characterised by the lack of accumumaltion of Chl a triplet state. In order to understand the mechanisms underlying the very efficient triplet-triplet transfer, we investigated LHCII by step-scan time-resolved FTIR spectroscopy. Upon excitation of LHCII carotenoids at 475 nm, the triplet decay was satisfactorily fitted with two components only using global analysis. The first component decays with a time constant of 20 µs, while the second component, which does not account for more than 10% of the signal, does not decay within the time window of the measurement (about 320 µs). Figure 9A displays the first decay-associated

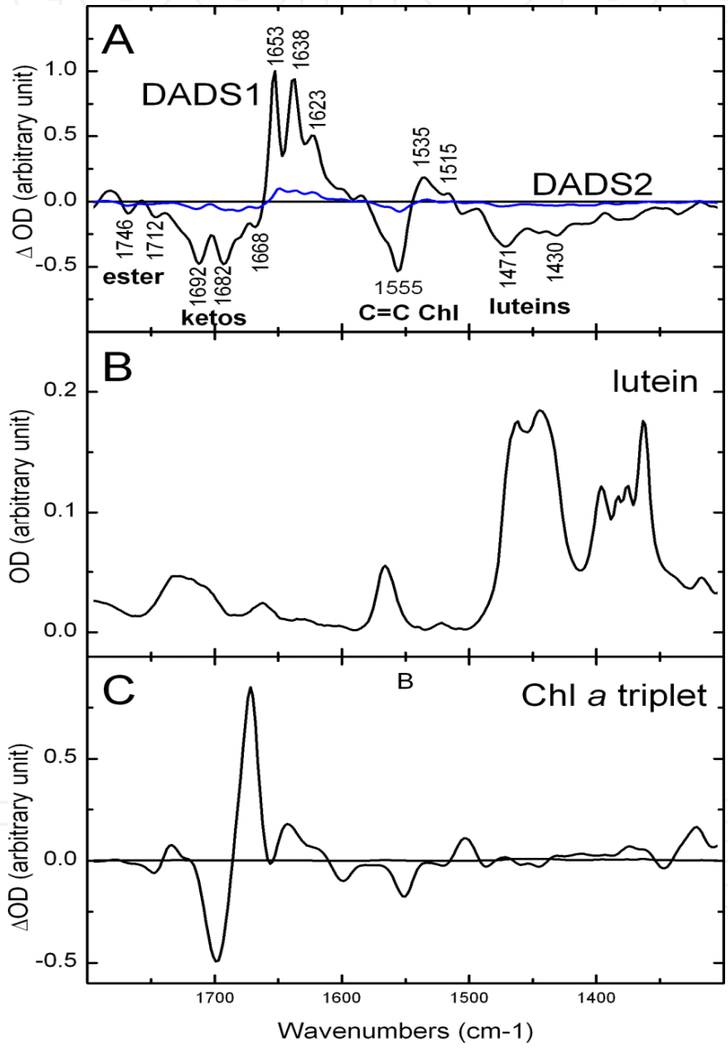

(A) The Decay-Associated Difference Spectra (DADS) have a 20 µs component (black trace, termed DADS1), with an amplitude of 90% (Lutein-Chls shared triplet) and a non-decaying component (blue trace termed DADS2) which has an amplitude of 10% (unquenched Chls). For clarity, the spectra have been normalized to the keto modes. For comparison, the FTIR of lutein (B) and Chl *a* (C) triplet (redrawn from (Bonetti, Alexandre et al. 2009)) in THF are also plotted

Fig. 9. Global analysis of step-scan FTIR data of LHCII excited at 475 nm showing the Lutein-Chls shared triplet state.

difference spectrum (DADS) normalized to the contribution of the keto group at 1653 cm^{-1}. Taking into account the time-resolved absorption data displayed above, the first decay-associated spectrum must be assigned to the carotenoid triplet (Fig. 9A, black spectrum and termed DADS1). In view of its long time the second one is attributed to unquenched Chl, *i.e.* a small proportion of triplet chlorophyll states which have not been transferred to the carotenoid molecules (Fig. 9A, blue spectrum and termed DADS2). It has already been observed that a small fraction of chlorophyll triplet may not be quenched by the carotenoid molecules (Mozzo, Dall'Osto et al. 2008). Considering the results of time-resolved absorption, DADS1 should contain positive contributions of the carotenoid triplet state and negative contributions of its ground state. Although such contributions clearly appear in the difference spectrum (region termed luteins), additional bands are obviously present in this spectrum. Indeed, no intense contribution in the higher frequency region is expected from lutein molecules (see Fig. 9B). On the contrary, in this region, DADS1 is typical of the spectrum of a chlorophyll triplet in solvent which is plotted in Fig. 9C for comparison (Breton, Nabedryk et al. 1999; Bonetti, Alexandre et al. 2009). The negative contributions around 1700 cm^{-1} represent bleaching of bands arising from the stretching modes of conjugated keto carbonyl groups. These groups, when conjugated with the Chl macrocycle, experience large downshifts upon triplet formation, which results in positive contributions at lower frequencies. Nevertheless, DADS1 has a lifetime characteristic of carotenoid triplets, and so we conclude that in LHCII these chlorophyll infrared modes decay with the same lifetimes as carotenoid modes. Then "sharing" of the triplet wavefunction is also observed for higher plants.

4. Comparison of higher plant and purple bacteria triplet state

Resonance Raman is a very sensitive and selective technique which allows access to the vibrational modes of molecules via inelastic scattering. In this section we describe the use of Resonance Raman to confirm the triplet delocalisation observed by step scan spectroscopy.

In solution, upon triplet state formation, the frequency of stretching modes of the conjugated C=C's of the molecule dramatically downshifts from 1522 to 1494 cm^{-1} for ß-carotene in tetrahydrofuran (THF; (Hashimoto, Koyama et al. 1991), (Fujiwara, Yamauchi et al. 2008)), or from 1529 to 1500 cm^{-1} for *all-trans* spheroidene in hexane (Mukai-Kuroda, Fujii et al. 2002). This reflects the localization of the triplet throughout the conjugated system (triplet high spin density "hot spot" is mainly in the centre of the conjugated system; ((Mukai-Kuroda, Fujii et al. 2002), (Di Valentin, Ceola et al. 2008)), which causes a reduction in the C=C bond order. The frequencies of the ν_1 resonance Raman bands observed in protein-bound carotenoid triplet spectra are reported in Table 2 and compared to those observed for triplet states of other carotenoids, including ß-carotene in solution and spheroidene bound to the bacterial reaction center. The downshift depends on the carotenoid configuration, and it is always larger in *cis* configurations ((Hashimoto, Koyama et al. 1991; Mukai-Kuroda, Fujii et al. 2002)). For rhodopin glucoside in LH2, this downshift of the band from 1517 to 1493 cm^{-1} is very similar to that observed for all-trans ß-carotene and spheroidene in solution (24 cm^{-1} *vs.* 23-25 cm^{-1}). In contrast, the observed downshifts for this band for both luteins in LHCII trimers, LHCII monomers, CP29 and CP43 are much smaller and in all cases close to 18 cm^{-1}, *i.e.* approximately 75% of the 23-25 cm^{-1}shift that is observed for all-*trans* carotenoid triplets in solution (see Table 2). Such a reduction of the ν_1

band's downshift reflects a dramatic alteration of the nature of the triplet state, which correlates very well with a reduction in the energy gap between the S_0/S_2 and T_1/T_n transitions observed for these carotenoids in LHCII (see Table 1; it is harder to determine this gap with precision for CP43 due to the larger number of carotenoid molecules in this complex).

Carotenoid (complex)	Number of C=C	$S_0 \rightarrow S_2$ (nm)	$T_1 \rightarrow T_n$ (nm)	ΔE (cm^{-1})
Neurosporene (LH2)	9	495	516	822
Spheroidene (LH2)	10	514	537	833
Rhodopin(LH2)	11	529	556	918
Lutein 1 (LHCII trimers)	10	494	506	480
Lutein 2 (LHCII trimers)	10	510	525	560
Lutein 1 and 2 (LHCII monomers, CP29)	10	494,494	508,505	558,441

Table 1. Electronic transitions of triplet carotenoid states in some LH2 complexes from purple bacteria (values obtained from (Angerhofer, Bornhaeuser et al. 1995)) and in higher plant LHCs prepared as trimers (lines 4 and 5, ((Peterman, Dukker et al. 1995), (Lampoura, Barzda et al. 2002), (Croce, Mozzo et al. 2007)) and monomers (line 6, ((Croce, Mozzo et al. 2007), (Peterman, Gradinaru et al. 1997)), and in CP29* (Croce, Mozzo et al. 2007).

Carotenoid	ν_1 (cm^{-1})	$\Delta\nu_1$ (cm^{-1})
LH2 rhodopin glucoside ground state	1517	24
LH2 rhodopin glucoside triplet	1493	
LHCII trimer Lutein1 ground state	1530	18
LHCII trimer Lutein 1 triplet	1512	
LHCII trimer Lutein 2 ground state	1526	18
LHCII trimer Lutein 2 triplet	1508	
LHCII monomer lutein ground state	1526	18
LHCII monomer lutein triplet	1508	
CP29 lutein ground state	1526	18
CP29 lutein triplet	1508	
CP43 lutein ground state	1522	18
CP43 lutein triplet	1504	
all-*trans* β-carotene singlet state in THF	1522	25
all-*trans* β-carotene triplet in THF	1497	
all-*trans*-spheroidene singlet state in *n*-hexane	1523	23
all-*trans*-spheroidene triplet in *n*-hexane	1500	

Table 2. Comparison of the position of ν_1 vibrational band in resonance Raman spectra of rhodopin glucoside in LH2, of lutein 1 (ground state of the latter from ref (Ruban, Berera et al. 2007)) and 2 in LHCII trimers and other carotenoid-containing complexes with all-*trans*-ß-carotene, and other carotenoids, in solution (taken from (Hashimoto, Koyama et al. 1991; Mukai-Kuroda, Fujii et al. 2002; Rondonuwu, Taguchi et al. 2004)).

5. Triplet state dynamic in purple bacteria, higher plant and algae, a molecular adaptation of the photoprotection mechanism

Recent time-resolved absorption spectra show that no chlorophyll *a* triplet is accumulated in LHCII and PCP while, on the other hand, the FTIR difference spectra strongly suggest the presence of Chl *a* contributions long after the initial excitation. In order to explain this apparent contradiction, the simplest hypothesis is that the triplet could be shared between carotenoid and chlorophyll molecules. This question has already been addressed in the literature. In order to explain the influence of the carotenoid triplet state on the absorption bands of the BChl molecules in LH complexes from purple bacteria, Angerhofer *et al.* proposed 'a small delocalization of the carotenoid triplet over an adjacent BChl molecule' (10). They also noted that the apparent rate of Bchl to carotenoid triplet-triplet transfer seems to correlate with how much the carotenoid triplet state is able to influence the BChl transition. However, it should be pointed out that in LH complexes from purple bacteria, the carotenoid and BChl molecules are very closely located (an essential condition for triplet/triplet transfer), and therefore they each constitute a sizeable part of the environment (or solvation) of the other. It would thus be expected that the dielectric changes following the appearance of the carotenoid triplet state would have a measurable influence on the BChl absorption transitions. Hence, these previous results do not formally demonstrate a sharing of the triplet. In contrast, the resonance Raman spectra reported in this chapter provides a direct and unambiguous measurement of the sharing of the triplet of the carotenoid molecule. Indeed, upon sharing, the carotenoid triplet should progressively loose its pure triplet character, and the Raman signature of this state should become intermediate between ground- and triplet-state. In the case of rhodopin glucoside in LH2 from *Rbl. acidophilus*, the downshift of the ν_1 band is quite similar to that of ß-carotene or spheroidene in solution. We may thus safely conclude that there is very little, if any, wavefunction sharing between carotenoid and BChl triplet states in the LH2 complex from *Rbl. acidophilus*.

In LHCs from higher plants, the presence of the triplet state of the lutein molecules is known to induce a net bleaching of the electronic absorption transition of the neighboring chlorophyll molecules (Peterman, Gradinaru et al. 1997). However, delocalization of the triplet was for a long time considered unlikely, due to the large energy gap between the triplet states of carotenoid and chlorophyll molecules (Peterman, Gradinaru et al. 1997). This position is challenged by time-resolved FTIR studies on PCP and LHCII, which demonstrate a co-existence of chlorophyll and carotenoid triplets throughout the entire triplet lifetime (Alexandre, Luhrs et al. 2007). In addition, resonance Raman spectroscopy provides additional information on the nature of the carotenoid triplet in these complexes. The sensitivity of the v_1 bands of the ground and triplet states is expected to exhibit similar responses to the environment. However, in LHCII we observe a reduction of the energy gap between the v_1 bands of the ground- and triplet states by more than 30%. This unambiguously indicates that the electronic state gained by the carotenoid has lost a fraction of its carotenoid triplet character, and consequently part of the triplet must be localized on another molecule. From the results of the step-scan time-resolved FTIR measurements (Fig. 9A), we may safely conclude that a neighbouring chlorophyll molecule is the acceptor of the carotenoid triplet. The fact that the same effect was found for both luteins to the same extent strongly substantiates this conclusion. Each lutein experiences a different protein environment (which induces the red-shift of the electronic transitions of lutein 2; (Liu, Yan et

al. 2004)), but is surrounded by a number of similarly-positioned chlorophylls. The fact that both luteins exhibit the same 75/25 sharing of the triplet is thus most easily explained as a result of the pseudo-symmetry of the position of these chlorophyll molecules (Liu, Yan et al. 2004). The same conclusion can be drawn for monomeric LHCII, CP29 and CP43.

A closer analysis of the recently-obtained time-resolved FTIR data obtained for the PCP peridinin triplet supports this analysis. In FTIR, the intensity and frequency of the bands arising from the vibrational modes of the triplet state should reflect the triplet sharing. Since most of the bands are distorted by the differential method and by overlapping contributions, an accurate determination of their precise intensity and frequency is difficult except in the case of well-isolated bands. In the case of LHCII (Fig. 9), no carotenoid band can safely be used for that purpose. In the PCP spectra, the band arising from the stretching mode of the lactone carbonyl of peridinin is well isolated and contributes at *ca.* 1745 cm^{-1}. From FTIR steady-state measurements of peridinin mixed with Chl *a* in THF (data not shown) the peridinin C=O lactone extinction coefficient was estimated to be similar to that of the Chl *a* C=O keto group. This allows us to estimate the extent of the 'triplet sharing' between peridinin and Chl *a*. From Fig. 8 the negative band area assigned to 9-keto C=O corresponds to about 25 and 40 % of the negative band area assigned to lactone C=O for A-PCP and H-PCP, respectively. Taking into account the similar C=O extinction coefficient of peridinin lactone C=O and Chl *a* 9-keto C=O, about 25 and 40 % of the ^{3}peridinin is shared with Chl *a* in A-PCP and H-PCP, respectively. This conclusion is in good agreement with the relative amplitude of the Q_y bleach as compared to the peridinin bleach of about 20 % in the

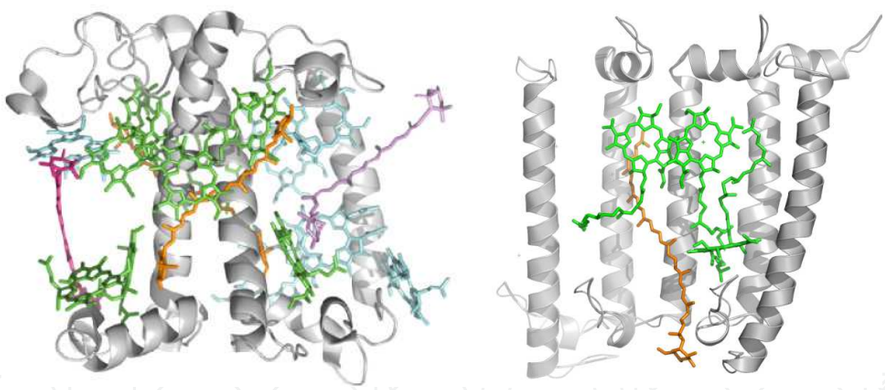

(A) A slice of the nonameric structure of the LH2 complex from *Rhodoblastus acidophilus* viewed in parallel with the membrane plane and from the outside of the protein. For clarity the central outer-helice, from three α/β-apoprotein dimers has been removed allowing the interaction of the Car (orange) with its nearest-neighbour Bchl *a* (green) molecules to be visualised. The contacts between Car and Bchl molecules essentially occur at the very end of the C=C conjugated chain of the carotenoid. Protein Data Bank accession number 1KZU. (B) View of a monomer of LHCII from *Spinacia oleracea* viewed in parallel with the membrane plane. The colours of the luteins (L1 and L2), neoxanthin (neo) and xanthophyll (xan) cycle carotenoids are orange, purple and magenta, respectively. The Chl *a* and Chl *b* molecules are coloured green and blue, respectively. The closest contacts between Chl *a* and luteins in LHCII occur at the middle of the C=C polyenic chain. Although the Chl molecules have a pseudo-symmetry within the monomer lutein 1 (L1) and lutein 2 (L2) experience a different protein environment. Protein Data Bank accession number 1RWT.

Fig. 10. The organisation of the (bacterio)chlorophyll and carotenoid molecules in LH2 and LHCII.

T-S spectra of A-PCP (Kleima, Hofmann et al. 2000). This estimate of a 25 and 40 % triplet sharing in A-PCP and H-PCP is also in line with the smaller observed bandshift of the carbonyl lactone for H-PCP (*i.e.* 20 cm^{-1} as compared to 25 cm^{-1} for A-PCP and 28 cm^{-1} for Per in THF).

Thus, in contrast to photosynthetic bacteria, our results provide compelling evidence of triplet sharing between carotenoid and chlorophyll molecules in plant and algal light-harvesting complexes. It is obviously tempting to try to unravel which molecular mechanisms may be at the origin of this difference. In LH2, contacts between carotenoid and bacteriochlorophyll molecules essentially occur at the very end of the C=C conjugated chain of the carotenoid (Fig. 10A and Ref. (McDermott, Prince et al. 1995)), and the minimum distance between these molecules is 3.42 Å (Prince, Papiz et al. 1997). In strong contrast, the closest contacts between Chl *a* and luteins in LHCII occur at the middle of the C=C polyenic chain (Fig. 10B), and the pigments are slightly more closely packed in these complexes. Taking into account the expected molecular structure of the carotenoid triplet state, the relative positioning of carotenoid and chlorophyll molecules in LHCII appears definitely more favourable for triplet sharing between these molecules

6. Conclusion

To summarize, our results clearly show that the nature of the triplet excited state of carotenoid molecules is fundamentally different in the LH2 from *Rbl. acidophilus* and the antenna isolated from spinach. In the former case, the triplet state is mainly (if not totally) localized on the rhodopin glucoside molecule. According to the work of Angerhofer *et al.*, (Angerhofer, Bornhaeuser et al. 1995), this is the case for the vast majority of light-harvesting proteins from purple photosynthetic bacteria. This localization of the triplet state is associated with a relatively slow triplet-triplet transfer between the BChl and carotenoid molecules, in the 20-200 ns time scale. In LHCII complexes from higher plants, there is a sharing of the triplet between luteins and their neighbouring chlorophylls. As this is also the case in CP43 and CP29, as well as in PCP, it is likely that this triplet sharing exists in all light-harvesting proteins from plants and algae. This delocalization is associated with an ultrafast transfer/equilibration of the triplet between the chlorophyll and carotenoid molecules, which results in the absence of any measurable accumulation of pure triplet chlorophyll in these complexes. However, the price to pay to avoid the accumulation of this species is that the triplet state is shared between the chlorophyll and the carotenoid lasts for several microseconds. Apparently such mechanism drags the energy of the shared triplet below that of singlet oxygen. The resultant decrease in the probability of production of singlet oxygen thereby optimizes photoprotection of these complexes. It is striking that this tuning of photoprotection was found only in those organisms which perform photosynthesis in the presence of large amounts of molecular oxygen. We propose that triplet sharing represents an adaptation of the molecular mechanisms of protection against photo-oxidative stress, associated with the evolution of oxygenic photosynthesis.

7. References

Alexandre, M. T., D. C. Luhrs, et al. (2007). "Triplet state dynamics in peridinin-chlorophyll-a-protein: a new pathway of photoprotection in LHCs?" Biophys J 93(6): 2118-28.

Angerhofer, A., F. Bornhaeuser, et al. (1995). "Optical and optically detected magnetic resonance investigation on purple photosynthetic bacterial antenna complexes." Chem. Phys. 194(2,3): 259-74.

Bautista, J. A., R. E. Connors, et al. (1999). "Excited state properties of peridinin: Observation of a solvent dependence of the lowest excited singlet state lifetime and spectral behavior unique among carotenoids." Journal of Physical Chemistry B 103(41): 8751-8758.

Bautista, J. A., R. G. Hiller, et al. (1999). "Singlet and triplet energy transfer in the peridinin-chlorophyll a protein from Amphidinium carterae." Journal of Physical Chemistry A 103(14): 2267-2273.

Bernhard, K. and M. Grosjean (1995). Infrared Spectroscopy. Carotenoids. G. Britton, S. Liaaen-Jensen and H. Pfander. Basel, Boston, Berlin, Birkhäuser Verlag. 1B.

Bonetti, C., M. T. A. Alexandre, et al. (2009). "Chl-a triplet quenching by peridinin in H-PCP and organic solvent revealed by step-scan FTIR time-resolved spectroscopy." Chemical Physics Excited State Dynamics in Light Harvesting Materials 357(1-3): 63-69.

Breton, J. (2001). "Fourier transform infrared spectroscopy of primary electron donors in type I photosynthetic reaction centers." Biochimica et Biophysica Acta (BBA) - Bioenergetics 1507(1-3): 180-193.

Breton, J., E. Nabedryk, et al. (1999). "FTIR study of the primary electron donor of photosystem I (P700) revealing delocalization of the charge in P700(+) and localization of the triplet character in (3)P700." Biochemistry 38(36): 11585-11592.

Brudler, R., R. Rammelsberg, et al. (2001). "Structure of the I1 early intermediate of photoactive yellow protein by FTIR spectroscopy." Nat Struct Biol 8(3): 265-70.

Carbonera, D., G. Giacometti, et al. (1996). "Carotenoid interactions in peridinin chlorophyll a proteins from dinoflagellates - Evidence for optical excitons and triplet migration." Journal of the Chemical Society-Faraday Transactions 92(6): 989-993.

Carbonera, D., G. Giacometti, et al. (1999). "Model for triplet-triplet energy transfer in natural clusters of peridinin molecules contained in Dinoflagellate's outer antenna proteins." Journal of Physical Chemistry B 103(30): 6357-6362.

Cogdell, R. J. and H. A. Frank (1987). "How Carotenoids Function in Photosynthetic Bacteria." Biochimica Et Biophysica Acta 895(2): 63-79.

Cogdell, R. J., T. D. Howard, et al. (2000). "How carotenoids protect bacterial photosynthesis." Phil. Trans. Royal Soc. London Ser B 355: 1345-1349.

Croce, R., M. Mozzo, et al. (2007). "Singlet and triplet state transitions of carotenoids in the antenna complexes of higher-plant Photosystem I." Biochemistry 46(12): 3846-3855.

Damjanovic, A., T. Ritz, et al. (1999). "Energy transfer between carotenoids and bacteriochlorophylls in a light harvesting protein." Physical Review E 59: 3293-3311.

Damjanovic, A., T. Ritz, et al. (2000). "Excitation transfer in the peridinin-chlorophyll-protein of *Amphidinium carterae*." Biophysical Journal 79(4): 1695-1705.

Dexter, D. L. (1953). "A theory of sensitized luminescence in solids." Journal of Chemical Physics 21: 834-850.

Di Valentin, M., S. Ceola, et al. (2008). "Pulse ENDOR and density functional theory on the peridinin triplet state involved in the photo-protective mechanism in the peridinin-chlorophyll a-protein from Amphidinium carterae." Biochim Biophys Acta 1777(3): 295-307.

Di Valentin, M., S. Ceola, et al. (2008). "Identification by time-resolved EPR of the peridinins directly involved in chlorophyll triplet quenching in the peridinin-chlorophyll a-protein from Amphidinium carterae." Biochim Biophys Acta 1777(2): 186-95.

Frank, H. A. and R. J. Cogdell (1996). "Carotenoids in photosynthesis." Photochemistry and Photobiology 63(3): 257-264.

Fujiwara, M. and M. Tasumi (1986). "Metal-sensitive bands in the Raman and infrared spectra of intact and metal-substituted chlorophyll a." Journal of Physical Chemistry 90(22): 5646-5650.

Fujiwara, M., Tasumi, M. (1986). "Resonance Raman and Infrared Studies on Axial Coordination to Chlorophylls-a and Chlorophylls-B Invitro." Journal of Physical Chemistry 90(2): 250-255.

Fujiwara, M., K. Yamauchi, et al. (2008). "Energy dissipation in the ground-state vibrational manifolds of ß-carotene homologues: a sub-20-fs time-resolved transient grating spectroscopic study." Phys Rev B 77: 205118-1-10.

Garczarek, F. and K. Gerwert (2006). "Functional waters in intraprotein proton transfer monitored by FTIR difference spectroscopy." Nature 439(7072): 109-12.

Gest, H. (2002). "History of the word photosynthesis and evolution of its definition." Photosynthesis Research 73(1-3): 7-10.

Groot, M. L., Breton, J., van Wilderen, L.J.G.W., Dekker, J.P., van Grondelle, R. (2004). "Femtosecond visible/visible and visible/mid-IR pump-probe study of the photosystem II core antenna complex CP47." Journal of Physical Chemistry B 108(23): 8001-8006.

Hartwich, G., C. Geskes, et al. (1995). "Fourier-Transform Infrared-Spectroscopy of Electrogenerated Anions and Cations of Metal-Substituted Bacteriochlorophyll-Alpha." Journal of the American Chemical Society 117(29): 7784-7790.

Hashimoto, H., Y. Koyama, et al. (1991). "S1 and T1 species of .beta.-carotene generated by direct photoexcitation from the all-trans, 9-cis, 13-cis, and 15-cis isomers as revealed by picosecond transient absorption and transient Raman spectroscopies." Journal of Physical Chemistry 95: 3072-3076.

Hashimoto, H., Y. Koyama, et al. (1991). "S1 and T1 Species of Beta-Carotene Generated by Direct Photoexcitation from the All-Trans, 9-Cis, 13-Cis, and 15-Cis Isomers as Revealed by Picosecond Transient Absorption and Transient Raman Spectroscopies." Journal of Physical Chemistry 95(8): 3072-3076.

Hiller, R. G., L. G. Crossley, et al. (2001). "The 15-kDa forms of the apo-peridinin-chlorophyll a protein (PCP) in dinoflagellates show high identity with the apo-32 kDa PCP forms, and have similar N-terminal leaders and gene arrangements." Mol Genet Genomics 266(2): 254-9.

Hofmann, E. (1999). Strukturanalyse der Lichtsammler Peridinin-Chlorophyll a-Proteine (PCPs) von Amphidinium carterae und Heterocapsa pygmaea. Dr. rer. nat. der Fakult¨at f¨ur Biologie Universit¨at Konstanz.

Hofmann, E., P. M. Wrench, et al. (1996). "Structural basis of light harvesting by carotenoids: Peridinin- chlorophyll-protein from Amphidinium carterae." Science 272(5269): 1788-1791.

Holt, N. E., J. T. M. Kennis, et al. (2003). "Carotenoid to chlorophyll energy transfer in light harvesting complex II from Arabidopsis thaliana probed by femtosecond fluorescence upconversion." Chemical Physics Letters 379: 305-313.

Ilagan, R. P., S. Shima, et al. (2004). "Spectroscopic properties of the main-form and high-salt peridinin-chlorophyll a proteins from Amphidinium carterae." Biochemistry 43(6): 1478-1487.

Katz, J. J., K. Ballschmiter, et al. (1968). "Electron paramagnetic resonance of chlorophyll-water aggregates." Proc Natl Acad Sci U S A 60(1): 100-7.

Kleima, F. J., E. Hofmann, et al. (2000). "Förster excitation energy transfer in peridinin-chlorophyll-a-protein." Biophys J 78(1): 344-53.

Kleima, F. J., Hofmann, E., Gobets, B., van Stokkum, I. H. M., van Grondelle, R., Diederichs, K., van Amerongen, H. (2000). "Forster excitation energy transfer in peridinin-chlorophyll-a-protein." Biophysical Journal 78(1): 344-353.

Kleima, F. J., M. Wendling, et al. (2000). "Peridinin chlorophyll a protein: Relating structure and steady-state spectroscopy." Biochemistry 39(17): 5184-5195.

Knoetzel, J. and L. Rensing (1990). "Characterization of the Photosynthetic Apparatus from the Marine Dinoflagellate Gonyaulax-Polyedra .1. Pigment and Polypeptide Composition of the Pigment-Protein Complexes." Journal of Plant Physiology 136(3): 271-279.

Kotting, C. and K. Gerwert (2005). "Proteins in action monitored by time-resolved FTIR spectroscopy." Chemphyschem 6(5): 881-8.

Krieger-Liszkay, A. (2005). "Singlet oxygen production in photosynthesis." J Exp Bot 56(411): 337-46.

Kristallovich, E. L., I. D. Shamyanov, et al. (1987). "Frequencies and Integral Intensities of Lactone and Ester Carbonyls of Natural Guaianolides." Khimiya Prirodnykh Soedinenii(6): 805-811.

Krueger, B. P., S. S. Lampoura, et al. (2001). "Energy transfer in the peridinin chlorophyll-a protein of Amphidinium carterae studied by polarized transient absorption and target analysis." Biophysical Journal 80(6): 2843-2855.

Krueger, B. P., G. D. Scholes, et al. (1998). "Calculation of couplings and energy-transfer pathways between the pigments of LH2 by the *ab initio* transition density cube method." Journal of Physical Chemistry B 102: 5378-5386.

Krueger, B. P., G. D. Scholes, et al. (1998). "Electronic excitation transfer from carotenoid to bacteriochlorophyll in the purple bacterium *Rhodopseudomonas acidophila*." Journal of Physical Chemistry B 102: 2284-2292.

Lampoura, S. S., V. Barzda, et al. (2002). "Aggregation of LHCII leads to a redistribution of the triplets over the central xanthophylls in LHCII." Biochemistry 41(29): 9139-9144.

Liu, Z., H. Yan, et al. (2004). "Crystal structure of spinach major light-harvesting complex at 2.72Å resolution." Nature 428(6980): 287-292.

Majerus, T., T. Kottke, et al. (2007). "Time-resolved FT-IR spectroscopy traces signal relay within the blue-light receptor AppA." Chemphyschem 8(12): 1787-9.

Mantele, W. G., A. M. Wollenweber, et al. (1988). "Infrared Spectroelectrochemistry of Bacteriochlorophylls and Bacteriopheophytins - Implications for the Binding of the Pigments in the Reaction Center from Photosynthetic Bacteria." Proceedings of the National Academy of Sciences of the United States of America 85(22): 8468-8472.

McDermott, G., S. M. Prince, et al. (1995). "Crystal structure of an integral membrane light-harvesting complex from photosynthetic bacteria." Nature 374(6522): 517-521.

Mimuro, M., N. Tamai, et al. (1990). "Characteristic Fluorescence Components in Photosynthetic Pigment System of a Marine Dinoflagellate, Protogonyaulax-

Tamarensis, and Excitation-Energy Flow among Them - Studies by Means of Steady-State and Time-Resolved Fluorescence Spectroscopy." Biochimica Et Biophysica Acta 1016(2): 280-287.

Mozzo, M., L. Dall'Osto, et al. (2008). "Photoprotection in the antenna complexes of photosystem II: role of individual xanthophylls in chlorophyll triplet quenching." J Biol Chem 283(10): 6184-92.

Mukai-Kuroda, Y., R. Fujii, et al. (2002). "Changes in molecular structure upon triplet excitation of all-trans-spheroidene in n-hexane solution and 15-cis-spheroidene bound to the photo-reaction center from Rhodobacter sphaeroides as revealed by resonance-Raman spectroscopy and normal-coordinate analysis." Journal of Physical Chemistry A 106(14): 3566-3579.

Nagae, H., T. Kakitani, et al. (1993). "Calculation of the Excitation Transfer-Matrix Elements between the S(2) or S(1) State of Carotenoid and the S(2) or S(1) State of Bacteriochlorophyll." Journal of Chemical Physics 98(10): 8012-8023.

Nagae, H., M. Kuki, et al. (2000). "Vibronic Coupling through the In-Phase, C=C Stretching Mode Plays a Major Role in the 2Ag- to 1Ag- Internal Conversion of all-trans--Carotene. pp 4155 - 4166;." Journal of Physical Chemistry A 104(18): 4155-4166.

Noguchi, T. (2002). "Dual Role of Triplet Localization on the Accessory Chlorophyll in the Photosystem II Reaction Center: Photoprotection and Photodamage of the D1 Protein." Plant and Cell Physiology 43(10): 1112-1116.

Noguchi, T., H. Hayashi, et al. (1990). "Frequencies of the Franck-Condon active a_g C=C stretching mode in the 2 $1A^-_g$ excited state of carotenoids." Chemical Physics Letters 175(3): 163-169.

Norris, B. J. and D. J. Miller (1994). "Nucleotide sequence of a cDNA clone encoding the precursor of the peridinin-chlorophyll a-binding protein from the dinoflagellate Symbiodinium sp." Plant Mol Biol 24(4): 673-7.

Okubo, T. and T. Noguchi "Selective detection of the structural changes upon photoreactions of several redox cofactors in photosystem II by means of light-induced ATR-FTIR difference spectroscopy." Spectrochimica Acta Part A: Molecular and Biomolecular Spectroscopy In Press, Corrected Proof.

Papagiannakis, E., J. T. M. Kennis, et al. (2002). "An Alternative carotenoid-to-bacteriochlorophyll energy transfer pathway in photosynthetic light harvesting." Proceedings of the National Academy of Sciences (USA) 99(9): 6017-6022.

Peterman, E. J., C. C. Gradinaru, et al. (1997). "Xanthophylls in light-harvesting complex II of higher plants: light harvesting and triplet quenching." Biochemistry 36(40): 12208-15.

Peterman, E. J. G., F. M. Dukker, et al. (1995). "Chlorophyll a and carotenoid triplet states in light-harvesting complex II of higher plants." Biophysical Journal 69(6): 2670-2678.

Premvardhan, L., E. Papagiannakis, et al. (2005). "The Charge-Transfer Character of the S0->S2 Transition in the Carotenoid Peridinin is revealed by Stark Spectroscopy." Journal of Physical Chemistry B 109: 15589-15597.

Prince, S. M., M. Papiz, . Z., et al. (1997). "Apoprotein structure in the LH2 complex from Rhodopseudomonas acidophila strain 10050: modular assembly and protein pigment interactions." J. Mol. Biol. 268(2): 412-423.

Ritz, T., A. Damjanovic, et al. (2000). "Efficient light harvesting through carotenoids." Photosynthesis Research 66(1-2): 125-144.

Rondonuwu, F. S., T. Taguchi, et al. (2004). "The energies and kinetics of triplet carotenoids in the LH2 antenna complexes as determined by phosphorescence spectroscopy." Chemical Physics Letters 384(4-6): 364-371.

Ruban, A. V., R. Berera, et al. (2007). "Identification of a mechanism of photoprotective energy dissipation in higher plants." Nature 450(7169): 575-8.

Salverda, J. M. (2003). Interacting pigments in light-harvesting complexes studied with nonlinear spectroscopy. Amsterdam, Vrije Universiteit.

Schopf, J. W. (1992). The oldest fossils and what they mean. Major events in the history of life. J. W. Schopf, Jones and Bartlett: 29-63.

Shreve, A. P., J. K. Trautman, et al. (1991). "Femtosecond Energy-Transfer Processes in the B800-850 Light- Harvesting Complex of Rhodobacter-Sphaeroides-2.4.1." Biochimica Et Biophysica Acta 1058(2): 280-288.

Song, P. S., P. Koka, et al. (1976). "Molecular Topology of Photosynthetic Light-Harvesting Pigment Complex, Peridinin-Chlorophyll-a-Protein, from Marine Dinoflagellates." Biochemistry 15(20): 4422-4427.

Van der Vos, R., D. Carbonera, et al. (1991). "Microwave and optical spectroscopy of carotenoid triplets in light-harvesting complex LHC II of spinach by absorbance-detected magnetic resonance." Appl. Magn. Res. 2: 179.

van Grondelle, R., J. P. Dekker, et al. (1994). "Energy-Transfer and Trapping in Photosynthesis." Biochimica Et Biophysica Acta-Bioenergetics 1187(1): 1-65.

van Stokkum, I. H., D. S. Larsen, et al. (2004). "Global and target analysis of time-resolved spectra." Biochim Biophys Acta 1657(2-3): 82-104.

Vaswani, H. M., C. P. Hsu, et al. (2003). "Quantum chemical evidence for an intramolecular charge-transfer state in the carotenoid peridinin of peridinin-chlorophyll- protein." Journal of Physical Chemistry B 107(31): 7940-7946.

Walla, P. J., P. A. Linden, et al. (2000). "Femtosecond dynamics of the forbidden carotenoid S-1 state in light-harvesting complexes of purple bacteria observed after two-photon excitation." Proceedings of the National Academy of Sciences (USA) 97: 10808-10813.

Zhang, J. P., R. Fujii, et al. (2000). "Mechanism of the carotenoid-to-bacteriochlorophyll energy transfer via the S_1 state in the LH2 complexes from purple bacteria." Journal of Physical Chemistry B 104(15): 3683-3691.

Zigmantas, D., R. G. Hiller, et al. (2004). "Effect of a conjugated carbonyl group on the photophysical properties of carotenoids." Physical Chemistry Chemical Physics 6(11): 3009-3016.

Zigmantas, D., R. G. Hiller, et al. (2002). "Carotenoid to chlorophyll energy transfer in the peridinin- chlorophyll-*a*-protein complex involves an intramolecular charge transfer state." Proceedings of the National Academy of Sciences of the United States of America 99(26): 16760-16765.

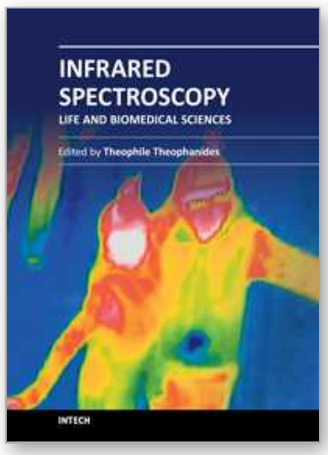

Infrared Spectroscopy - Life and Biomedical Sciences
Edited by Prof. Theophanides Theophile

ISBN 978-953-51-0538-1
Hard cover, 368 pages
Publisher InTech
Published online 25, April, 2012
Published in print edition April, 2012

This informative and state-of-the art book on Infrared Spectroscopy in Life sciences designed for researchers, academics as well as for those working in industry, agriculture and in pharmaceutical companies features 20 chapters of applications of MIRS and NIRS in brain activity and clinical research. It shows excellent FT-IR spectra of breast tissues, atheromatic plaques, human bones and projects assessment of haemodynamic activation in the cerebral cortex, brain oxygenation studies and many interesting insights from a medical perspective.

How to reference
In order to correctly reference this scholarly work, feel free to copy and paste the following:

Alexandre Maxime and Rienk van Grondelle (2012). Time-Resolved FTIR Difference Spectroscopy Reveals the Structure and Dynamics of Carotenoid and Chlorophyll Triplets in Photosynthetic Light-Harvesting Complexes, Infrared Spectroscopy - Life and Biomedical Sciences, Prof. Theophanides Theophile (Ed.), ISBN: 978-953-51-0538-1, InTech, Available from: http://www.intechopen.com/books/infrared-spectroscopy-life-and-biomedical-sciences/time-resolved-ftir-difference-spectroscopy-reveals-the-structure-and-dynamics-of-carotenoid-and-chlo

INTECH
open science | open minds

InTech Europe
University Campus STeP Ri
Slavka Krautzeka 83/A
51000 Rijeka, Croatia
Phone: +385 (51) 770 447
Fax: +385 (51) 686 166
www.intechopen.com

InTech China
Unit 405, Office Block, Hotel Equatorial Shanghai
No.65, Yan An Road (West), Shanghai, 200040, China
中国上海市延安西路65号上海国际贵都大饭店办公楼405单元
Phone: +86-21-62489820
Fax: +86-21-62489821

IntechOpen